Chemical Engineering Journal 134 (2007) 106–110

Chemical Engineering Journal

www.elsevier.com/locate/cej

n-Hexane skeletal isomerization over sulfated zirconia catalysts with different Lewis acidity

G.G. Volkova*, S.I. Reshetnikov, L.N. Shkuratova, A.A. Budneva, E.A. Paukshtis

Boreskov Institute of Catalysis, Pr. Akademika Lavrentieva 5, Novosibirsk 630090, Russia

Abstract

The *n*-hexane skeletal isomerization over Pt/SO_4^{2-}/Al_2O_3/ZrO_2 catalysts with different density of Lewis acid sites has been studied in a fixed-bed reactor. The acidity of the catalysts was characterized by FTIR spectroscopy of low temperature CO adsorption. The calculation of the rate constants, characterizing the catalyst activity and selectivity was performed on the base of mathematical model of plug flow reactor. It was shown that the rate of hexane isomerization is mainly determined by the density of Lewis acid sites on the surface of sulfated zirconia catalysts: rate constant of *n*-hexane isomerization for catalyst with Lewis acidity 250 μmol g^{-1} is four-fold as that for catalyst with concentration of Lewis acid sites 150 μmol g^{-1} and the rate constant of desired product (2,2-dimethylbutane) formation is also higher by two times.

Keywords: Isomerization; Lewis acid; Sulfated zirconia

1. Introduction

Naphtha isomerization is a simple and cost effective technology for increasing octane number of gasoline. Skeletal isomerization of light naphtha is composed mainly of conversion of *n*-pentane and *n*-hexane into branched alkanes. Multiply branched alkanes have higher octane number than mono-methyl alkanes, and are preferentially produced at low temperature subject to chemical equilibrium. Recently new acid catalysts based on sulfated zirconia (SZ) have been developed and successfully commercialized by UOP LLC [1–3]. These catalysts offer a nice alternative for the corrosive halogen-containing solid acids for light naphtha skeletal isomerization at low temperature. By the large demand of desired isomerization products development of new more active catalysts has been continued [4].

It is known that activity of the SZ catalysts significantly depends on preparation procedure, the activity of the catalysts with the same structure and equal in sulfate content may differ by one order of magnitude [5]. Many researchers try to reveal the critical differences determining the variation in catalytic activity and to recognize the important characteristics of the active SZ catalyst: is that Bronsted or Lewis acidity or both of them or other parameter [6–18]. In the last years some authors emphasize the participation of Lewis acid sites in the reaction mechanism for alkane isomerization [11–13]. But there are no direct arguments for this idea yet. Here we try to give the proofs of the dependence between activity of SZ catalysts and their Lewis acidity. Maximum densities of Lewis acid sites on SZ catalysts presented in literature were 90–121 μmol g^{-1} [19–21]. Our group has developed SZ catalysts with higher density of Lewis acid sites—200–250 μmol g^{-1} [22].

The aim of this work was to investigate the *n*-hexane skeletal isomerization over Pt/SO_4^{2-}/Al_2O_3/ZrO_2 catalysts with different density of Lewis acid sites.

2. Experimental

2.1. Catalysts preparation

Zirconium–aluminium hydroxides were precipitated from the aqueous solution of zirconium oxynitrate and aluminium nitrate by ammonium hydroxide at the variation of pH from 7 to 11.5. The obtained solids were washed with distilled water until the complete elimination of nitrate ions. The zirconium–aluminium hydroxides were sulfated with H_2SO_4 and calcinated at 650 °C. Platinum was loaded by incipient wetness impregnation with an H_2PtCl_6 solution. The final catalysts were calcined at 500 °C for 3 h [22]. Catalysts composition is Pt = 0.3%, SO_4 = 6%, Al_2O_3 = 2.5%. BET surface area was 100–120 m^2 g^{-1}.

---

* Corresponding author.
E-mail address: ggvolkova@catalysis.ru (G.G. Volkova).

doi:10.1016/j.cej.2007.03.079

2.2. FTIR characterization

FTIR spectroscopy was applied to determine the acidity of the catalysts by monitoring the adsorption of CO (adsorbance band at 2150–2175 cm^{-1} for Bronsted and 2185–2200 cm^{-1} for Lewis acid sites). The samples were pressed into self-supporting wafers containing of 15–20 $mg\,cm^{-2}$ material. Samples were reduced by hydrogen in situ in IR sell at the temperature 200 °C then degassed at 200 °C and then cooled to the −173 °C and treated with low doses of CO. The spectra were recorded in the range of 2000–2300 cm^{-1} with 4 cm^{-1} resolution using Shimadzu FTIF-8300 spectrometer.

The number of sites of each type was calculated by fitting the data to equation $N = A/\rho A_o$, where A is the integrated intensity of band, ρ the mass of material ($g\,cm^{-2}$) and A_o is the molar integrated absorption coefficient equal to 0.8 $cm\,\mu mol^{-1}$ for band 2185–2200 cm^{-1} and 2.6 $cm\,\mu mol^{-1}$ for the band 2150–2175 cm^{-1}. Procedure for determination of A_o is described in ref. [23].

2.3. Activity measurements

Catalysts were evaluated in a fixed-bed flow reactor with a gas chromatography analysis on line. Reaction conditions were varied: H_2/C_6H_{14} ratio from 2/1 to 5/1, pressure from 0.3 to 1.5 MPa, temperature from 180 to 250 °C. Prior to reaction, samples were reduced in situ at 200 °C (heating rate 2 °C min^{-1}) in stream of 2% H_2–He for 2 h.

3. Results and discussion

3.1. FTIR study

IR spectra of adsorbed CO on sulfated zirconia catalysts (Fig. 1) revealed bands characteristic of both Lewis (2185–2200 cm^{-1}) and Bronsted (2150–2175 cm^{-1}) forms of adsorption. Table 1 collects the acidity data calculated from FTIR spectra of CO adsorption.

A three to five-fold variation in concentration of the Lewis acid sites is apparent across the range of samples. At the same time density of Bronsted acid sites lightly varies.

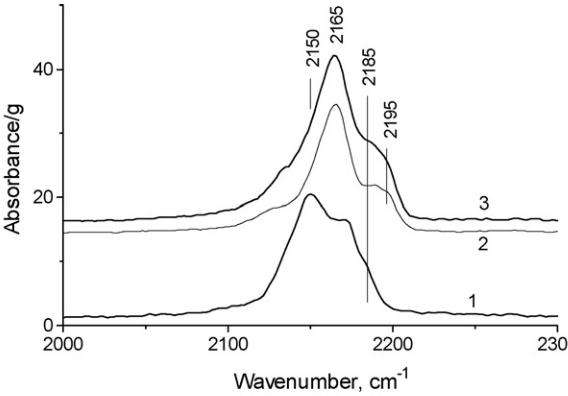

Fig. 1. FTIR spectra of adsorbed CO at temperature 100 K and pressure 10 Torr on $Pt/SO_4^{2-}/Al_2O_3/ZrO_2$ catalysts: (1) SZ-1; (2) SZ-2; (3) SZ-3.

Table 1
FTIR spectroscopy data of CO adsorption

Catalysts	νCO (cm^{-1})	Lewis acid sites ($\mu mol\,g^{-1}$)	Bronsted acid sites ($\mu mol\,g^{-1}$)
SZ-1, pH 7	2185	50	
	2175		85
	2150		140
SZ-2, pH 10	2200–2190	150	
	2175–2165		140
SZ-3, pH 11.5	2200–2190	250	
	2175–2165		170

The lowest concentration of Lewis acid sites equal 50 $\mu mol\,g^{-1}$ was observed for catalyst 1 precipitated at pH 7. Catalysts precipitated at pH 10 and 11.5 were characterized by the density of Lewis acid sites of 150 and 250 $\mu mol\,g^{-1}$.

It is known that acid strength may be characterized by spectroscopic identification of the interaction between acid site and a weak base. In the adsorption of CO molecule on Lewis acid site electrons in the antibonding level of the C≡O bond become stabilized, i.e., C≡O bond becomes stronger [24]. The resulting shift of the IR band to higher wave number was used by Knozinger and co-workers as a measure of acid strength [25–27]. So the strength of Lewis acid sites for catalysts 2 and 3 which characterized by 2190–2200 cm^{-1} is higher than those for catalyst 1 with wave numbers 2185 cm^{-1}. The catalysts 2 and 3 with highest and equal strength and different concentration of Lewis acid sites 150 and 250 $\mu mol\,g^{-1}$ were chosen for further detail kinetic investigation.

3.2. Kinetic study

Study of the kinetics of isomerization of the *n*-hexane on solid superacids has shown that it is possible to divide process into three stages [28]. The first, the fastest stage, is formation of 3-methyl pentane (3MP) from 2-methyl pentane (2MP), and then, 2,3-methyl butane (2,3DMB) formation up to thermodynamic equilibrium. The reactions of the isomerization of *n*-hexane and the formation of 2,2-methyl butane (2,2DMB) has the comparable rates. Third stage is the side products formation. The same results were obtained for hexane isomerization over HF-SbF_5 catalyst [29].

For the kinetic analysis the following reaction network (Scheme 1) was used:

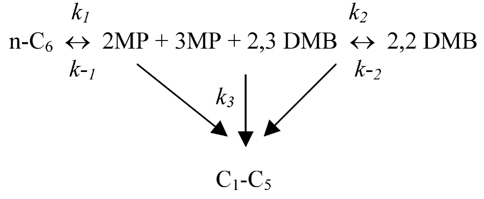

Rate of isomerization is influenced by many factors such as initial ratio of reagents, reaction conditions and so on. However, it was noted in many papers that the reactions are pseudo-first order in reagents.

The calculation of the rate constants, characterizing the catalyst activity and selectivity, was performed on the base of mathematical model of a plug flow reactor:

$$\frac{dC_1}{d\tau} = -k_1C_1\left(1-\frac{C_2}{C_1K_{e1}}\right),$$

$$\frac{dC_2}{d\tau} = k_1C_1\left(1-\frac{C_2}{C_1K_{e1}}\right) - k_2C_2\left(1-\frac{C_3}{C_2K_{e2}}\right) - k_3C_2,$$

$$\frac{dC_3}{d\tau} = k_2C_2\left(1-\frac{C_3}{C_2K_{e2}}\right),$$

$$\frac{dC_4}{d\tau} = k_3C_2,$$

where C_1 is the mole fraction of *n*-hexane, C_2 the 2MP + 3MP + 2,3 DMB, C_3 the 2,2 DMB, C_4 the cracking products, τ the contact time, k_i,k_{-i} the rate constants of direct and reverse reactions of *n*-hexane isomerisation and 2,2 DMB formation and K_{ei} is the equilibrium constants.

To solve the system of differential equations, which describes the balance correlation of the components in the gas phase, we used the semi-implicit method of Runge–Kutta to integrate a set of the stiff ordinary differential equations.

The calculation of the kinetic rate constants was made in the following order:

1. Thermodynamic equilibration was calculated based on value of entropy and enthalpy of *n*-hexane, 2MP, 3MP, 2,3 DMB, 2,2 DMB and equilibrium concentrations of above mention components were obtained for each temperature at the range 150–250 °C (Fig. 2).
2. Equilibrium constants for all stages of Scheme 1 were determined based on equilibrium concentrations.
3. Rate constants were determined on the basis of description of the experimental data at the given equilibrium constants.

The kinetic rate constants and activation energies were determined. Figs. 3 and 4 present the experimental and calculated data

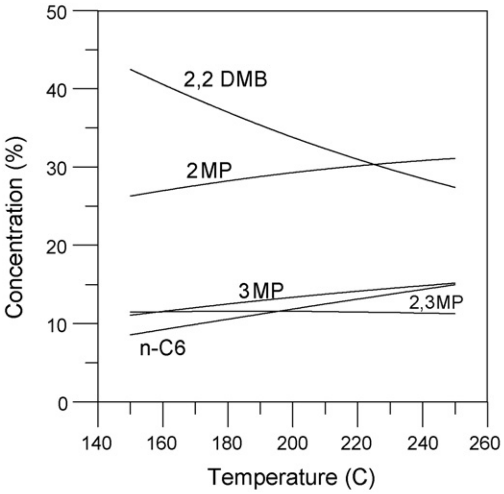

Fig. 2. Dependence of the equilibrium concentrations of n-C_6 isomerization products on temperature.

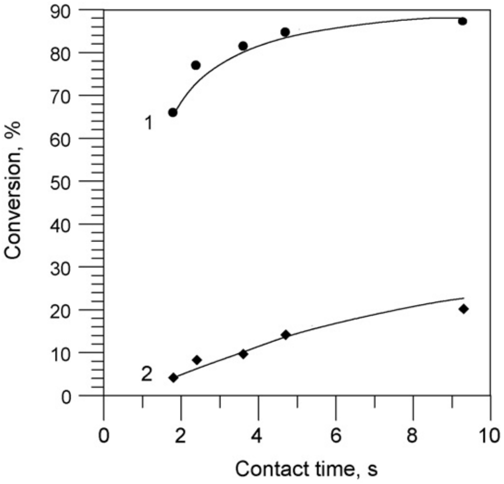

Fig. 3. The dependence of *n*-hexane conversion (1) and the 2,2 DMB concentration (2) on contact time for SZ-2 catalysts (points: experiment; lines: modeling). $P = 1$ MPa, $H_2/nC_6 = 5$.

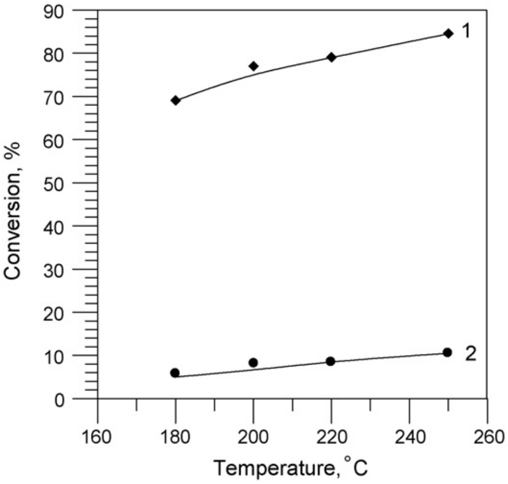

Fig. 4. The dependence of *n*-hexane conversion (1) and the 2,2 DMB concentration (2) on temperature for SZ-2 catalysts (points, experiment; lines, modeling). $P = 1$ MPa, $H_2/nC_6 = 5$.

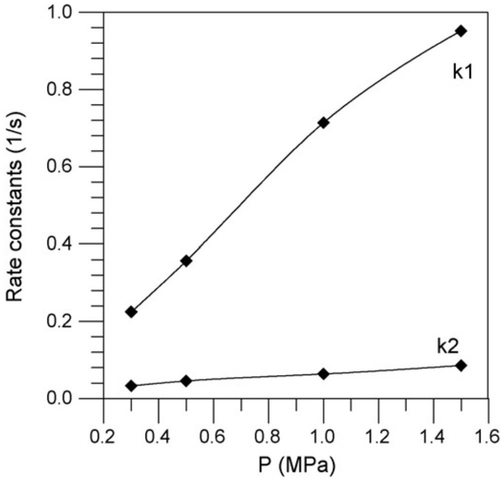

Fig. 5. The rate constans of *n*-hexane isomerization (k_1) and 2,2 DMB formation (k_2) vs. pressure for SZ-2 catalyst, calculated from description of experimental data (points). $T = 200$ °C, $H_2/nC_6 = 5$.

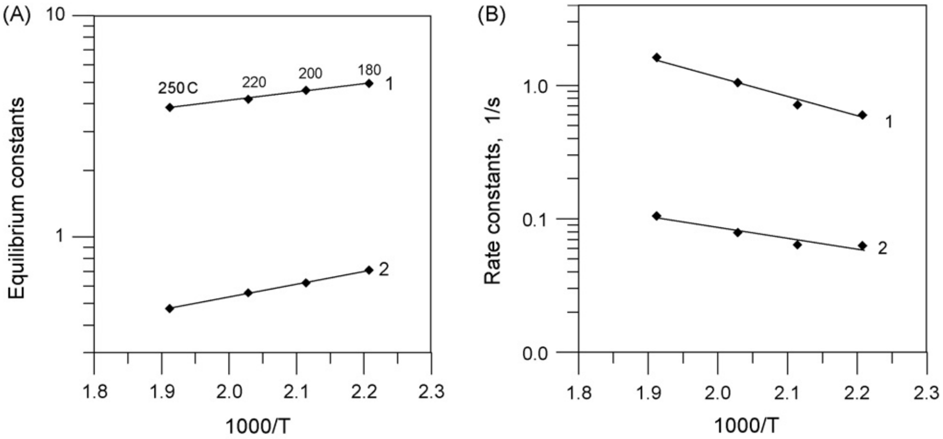

Fig. 6. Arrhenius plot of equilibrium constants (A) and rate constants (B) for SZ-2 catalyst: (1) step of n-hexane izomerization; (2) step of 2,2 DMB formation.

obtained at various contact times and temperatures for SZ-2 catalyst. It can be seen that the results of mathematical modeling are in good agreement with experimental data.

Analogously the experimental results obtained at various pressures over SZ-2 catalyst were modeling and presented at Fig. 5. The model was found to fit experimental data reasonably well.

Activation energies of direct (28 and 14.2 kJ mol^{-1}) and reverse reactions (35 and 25.5 kJ mol^{-1}) were estimated from the Arrhenius plot of equilibrium constants and rate constants of direct reactions for SZ-2 catalyst (Fig. 6, Scheme 1).

Comparison of experimental and calculated data for two catalysts with different density of Lewis acid sites is presented in Table 2. Experimental results were obtained under the same reaction conditions.

The data presented in Table 2 show that rate constant of n-hexane isomerization (k_1) for catalyst 3 is four-fold as those for catalyst 2, and k_2 which characterized the rate of desired product (2,2DMB) formation for catalyst 3 (Lewis acidity 250 μmol g^{-1}) is more than two higher than for catalyst 2 (Lewis acid sites 150 μmol g^{-1}). From these data it may be concluded that the rate of n-hexane isomerization is mainly determined by the density of Lewis acid sites on the surface of sulfated zirconia catalysts.

Thus, we experimentally demonstrated the key role of Lewis acid sites in the skeletal isomerisation of alkanes on sulfated zirconia catalysts as it was suggested by many groups of researchers [11–13,30,31]. At the same time the increase of catalysts activity exceeded the rise in concentration of Lewis acid sites. It was shown that Bronsted acid sites readily convert into Lewis acid sites upon heating [32,33]. In our case this phenomena hardly affects the activity rise. It may be explained by bifunctional nature of catalysts (metal–acid) usually required for alkane isomerisation, in which metal sites catalyze alkane dehydrogenation and acid sites catalyze skeletal isomerization of alkenes [34]. In the literature there are several identifications for these metal–acid pair species. Pt presence may produced “compressed bifunctional metal–acid sites” [35] or metal (or metal oxide) species may be distinguished into two parts associated or nonassociated with acid sites [36]. For the Pt/SO_4/Al_2O_3/ZrO_2 catalyst we have observed that increase in Lewis acid sites from 150 to 250 μmol g^{-1} led to four-fold increase in isomerization rate constant. It possibly means that amount of Pt species associated with Lewis acid sites increased four times too.

Table 2
Experimental and calculated kinetic data for n-hexane skeletal isomerization over SZ-2 and SZ-3 catalysts, pressure 0.3 MPa, temperature 200 °C

Parameters	SZ-2 (Lewis acid sites 150 μmol g^{-1})		SZ-3 (Lewis acid sites 50 μmol g^{-1})	
	Experiment	Calculation	Experiment	Calculation
2,2DMB (%)	1.5	1.5	4.6	4.5
2MP + 3MP + 2.3DMB (%)	35.1	34.8	59.86	60.0
n-C_6 conversion (%)	40.3	40.2	69.2	69.3
Rate constants (s^{-1})				
k_1		0.224		0.909
k_{-1}		0.048		0.20
k_2		0.033		0.073
k_{-2}		0.053		0.12
	n-Hexane (h^{-1})	2.79	4.68	
	H_2:n-C_6	2.09	1.87	

4. Conclusion

The skeletal isomerization of *n*-hexane was carried out in a fixed bed reactor over sulfated zirconia catalysts with different density of Lewis acid sites and with about the same Bronsted acidity. The key role of Lewis acidity for the activity and selectivity of the $Pt/SO_4^{2-}/Al_2O_3/ZrO_2$ catalysts was experimentally revealed.

References

[1] T. Kimura, Catal. Today 81 (2003) 57.

[2] S.A. Gembicki, Stud. Surf. Sci. Catal. 130 (2000) 147.

[3] UOP website: www.uop.com.

[4] US Patent 5,036,035 (1991), US Patent 6,495,733 (2002), US Patent 6,448,198, (2002) US Patent 5,629,257 (1997), US Patent 6,706,659 (2003).

[5] X. Li, K. Nagaoka, L.J. Simon, J.A. Lercher, S. Wrabetz, F.C. Jentoft, C. Breitkopf, S. Matysik, H. Paap, J. Catal. 230 (2005) 214.

[6] X. Yang, R.E. Jentoft, F.C. Jentoft, Catal. Lett. 106 (2006) 195.

[7] R.W. Stevens Jr., S.S.C. Chuang, B.H. Davis, Appl. Catal. 252 (2003) 57.

[8] E. Garcia, M.A. Volpe, M.L. Ferreira, E. Rueda, J. Mol. Catal. 201 (2003) 263.

[9] K. Arata, H. Matsuhashi, M. Hino, H. Nakamura, Catal. Today 81 (2003) 17.

[10] T. Lei, J.S. Xu, W.M. Hua, Z. Gao, Appl. Catal. A: Gen. 192 (2000) 181.

[11] J. van Gestel, V.T. Nghiem, D. Guillaume, J.P. Gilson, J.C. Duchet, J. Catal. 212 (2002) 173.

[12] J.C. Duchet, D. Guillaume, A. Monnier, C. Dujardin, J.P. Gilson, J. van Gestel, G. Szabo, P. Nascimento, J. Catal. 198 (2001) 328.

[13] H. Matsuhashi, H. Shibata, H. Nakamura, K. Arata, Appl. Catal. 187 (1999) 99.

[14] J.B. Laizet, A.K. Soiland, J. Leglise, J.C. Duchet, Top. Catal. 10 (2000) 89.

[15] S. Furuta, Appl. Catal. 251 (2003) 285.

[16] R. Barton, F. Lonyi, J. Engelhardt, J. Valyon, Top. Catal. 10 (2000) 79.

[17] C.R. Vera, J.C. Yori, C.L. Pieck, S. Irusta, J.M. Parera, Appl. Catal. 240 (2003) 161.

[18] J.A. Moreno, G. Poncelet, Appl. Catal. 210 (2001) 151.

[19] D.J. Rosenberg, J.A. Anderson, Catal. Lett. 83 (2002) 59.

[20] E.A. Paukshtis, V.K. Duplyakin, V.P. Finevich, A.V. Lavrenov, V.L. Kirillov, L.I. Kuznetsova, V.A. Likholobov, B.S. Bal'zhinimaev, Stud. Surf. Sci. Catal. 130 (2000) 2543.

[21] L. Zanibelli, A. Carati, C. Flego, R. Millini, Stud. Surf. Sci. Catal. 143 (2002) 813.

[22] G.G. Volkova, L.N. Shkuratova, L.S. Egorova, E.A. Paukshtis, A.A. Budneva, S.I. Reshetnikov, G.N. Kustova, V.K. Duplyakin, V.A. Likholobov, Russian Patent 2,273,517 (2006).

[23] E.A. Paukshis, IR Spectroscopy for Heterogeneous Acid–Base Catalysis, Nauka, Novosibirsk, 1992 (in Russian).

[24] W.M.H. Sachtler, in: A.F. Carley, Ph.R. Davies, G.J. Hutchings, M.S. Spencer (Eds.), Surface Chemistry and Catalysis, Kluwer Academic/Plenum Pablishers, New York, 2002, p. 208.

[25] M. Zaki, H. Knozinger, J. Catal. 119 (1989) 311.

[26] K.M. Neyman, P. Strodel, S.Ph. Ruzankin, N. Schlensorg, H. Knozinger, N. Rosch, Catal. Lett. 10 (1995) 273.

[27] A. Ponchel, F. Anderle, W. Daniell, H. Knozinger, Res. Chem. Intermed. 29 (2003) 705.

[28] D.M. Brouwer, J.M. Olderik, Reac. Trav. Chim. 87 (1968) 721.

[29] R. Bonifay, B. Torek, Bull. Soc. Chim. Fr. N 11–12 (1977) 1057–1065.

[30] P. Nascimento, C. Akratopoulou, M. Oszagyan, G. Travers, J.F. Joly, J.C. Vedrine, in: L. Guczi, F. Solimosi, P. Ttnyi (Eds.), New Frontiers in Catalysis, Elsevier, Amsterdam, 1993, p. 1185.

[31] M. Signoretto, F. Pinna, F. Strukul, P. Chies, G. Cerrato, S. Di Ciero, C. Monterra, J. Catal. 167 (1997) 522.

[32] G.D. Yadav, J.J. Nair, Microporous Macroporous Mater. 33 (1999) 1.

[33] A. Corma, Chem. Rev. 95 (1995) 559.

[34] E. Iglesia, S.L. Soled, G.M. Kramer, J. Catal. 144 (1993) 238.

[35] G. Resofszki, M. Muhler, S. Sprenger, U. Wild, Z. Paal, Appl. Catal. 240 (2003) 71.

[36] Y. Xu, X. Bao, L. Lin, J. Catal. 216 (2003) 386.